Hydrophobic W10O324-/silica photocatalyst for toluene oxidation in water system

Hydrophobic $W_{10}O_{32}^{4-}$/silica photocatalyst for toluene oxidation in water system

Alessandra Molinari,*[a] Giuliana Magnacca,[b] Gabriele Papazzoni,[a] Andrea Maldotti*[a]

[a] Dipartimento di Scienze Chimiche e Farmaceutiche, Via Luigi Borsari 46, Università di Ferrara, 44121 Ferrara, Italia; e-mail mna@unife.it, mla@unife.it Tel +390532455147, Fax +390532240709

[b] Università di Torino, Dipartimento di Chimica, NIS Centre of Excellence, via P. Giuria 7, 10125 Torino, Italia.

Abstract

A new photocatalyst ($Na_4W_{10}O_{32}/SiO_2$/BTESE) has been prepared by simultaneous hydrolysis of tetraethyl orthosilicate (TEOS) and 1,2-bis(triethoxysilyl)ethane (BTESE) in the presence of $Na_4W_{10}O_{32}$. This material is able to scavenge and accumulate significative amounts of toluene from water solutions saturated with the hydrocarbon. This is due to its large specific surface area, micro and mesoporosity, and, above all, to the high hydrophobicity of its surface. Moreover, photoexcited $Na_4W_{10}O_{32}/SiO_2$/BTESE shows a very strong oxidizing ability, allowing an almost complete mineralization of toluene to CO_2 through the formation and reactivity of $OH^{\bullet}$ radicals. On the contrary, $Na_4W_{10}O_{32}$ dissolved in homogeneous solution converts only a very limited amount of toluene to CO_2, indicating that textural effects critically affect the photooxidation properties of the decatungstate. At the end of a cycle of reaction, $Na_4W_{10}O_{32}/SiO_2$/BTESE is reusable without any loss of activity opening to the development of new efficient and stable photocatalytic systems addressed to clean wastewater containing aromatic hydrocarbons.

Keywords: photocatalysis, pollution abatement, polyoxoanion, toluene oxidation

1. Introduction

Polyoxotungstates (POTs) continue to be the object of intense interest in oxidative photocatalysis [1-4].This research topic moves towards a "sustainable chemistry" opening to new reaction routes either for syntheses or for wastewater treatments that require O_2 as available and cheap oxidant, mild conditions of temperature and pressure, and use of light as renewable source of energy. Among the POTs investigated, the decatungstate anion $W_{10}O_{32}^{4-}$ presents an absorption spectrum that partially overlaps the UV solar emission, opening the possibility to carry out fine solar-assisted applications [5-9].

The proposed mechanism for decatungstate-based photocatalysis involves absorption of light by the polyanion ground state leading to an oxygen to metal charge-transfer excited state

($W_{10}O_{32}^{4-*}$) [6, 10] that decays in few picoseconds to a very reactive transient species (wO). This species has an oxyradical-like character with a longer lifetime (about 50 nanoseconds) and is able to oxidize many substrates to their corresponding radicals with the simultaneous formation of the mono-reduced form of the decatungstate ($W_{10}O_{32}^{5-}$) [3, 6]. Oxidation of $W_{10}O_{32}^{5-}$ by O_2 restores the starting $W_{10}O_{32}^{4-}$ and causes dioxygen reductive activation to peroxy species. Moreover, in aqueous solutions, the formation of highly reactive hydroxyl radicals through the direct reaction between photoexcited polyoxoanions and water was demonstrated [1, 11-14]: this process can be described by Eq. 1.

$$wO + H_2O \longrightarrow W_{10}O_{32}^{5-} + OH^{\bullet} + H^{+} \qquad (1)$$

In recent years, heterogenization of $W_{10}O_{32}^{4-}$ on organic and inorganic solid matrices has progressed significantly, and great attention is being devoted to design new photoactive materials in order to control efficiency and selectivity of oxidation processes through the control of the local environment surrounding the photoactive decatungstate cluster [13-27]. More specifically, micro and mesoporous materials, and the appropriate ratio of surface hydrophobic/hydrophilic character are considered helpful for improving the enrichment of substrates in the proximity of the POT.

We reported recently data concerning the entrapment of $Na_4W_{10}O_{32}$ in a silica matrix by hydrolysis of tetraethylorthosilicate (TEOS) for obtaining a good photocatalytic material ($Na_4W_{10}O_{32}/SiO_2$). This system photogenerated hydroxyl radicals that, in turn, were able to induce alcohols oxidation [13, 14]. In the present work, the new material $Na_4W_{10}O_{32}/SiO_2$/BTESE was prepared through simultaneous hydrolysis of TEOS and 1,2-bis(triethoxysilyl)ethane (BTESE). In line with literature data on related systems, this procedure allows to obtain silica characterized by high surface hydrophobicity [28, 29]. This was already proved for chromium-modified mesoporous silica, where the hydrophobization enhanced the photoactivity of chromate species in the oxidation of cyclohexane [30, 31].

The photocatalytic activity of both $Na_4W_{10}O_{32}/SiO_2$ and $Na_4W_{10}O_{32}/SiO_2$/BTESE is here investigated for the first time in the oxidation of toluene in aqueous solution. Toluene is a very noxious organic compound that can be found in several industrial waste effluents, and its photocatalytic abatement in aqueous systems has been previously carried out with irradiated TiO_2 [32]. Particular attention is devoted to the effect of the organoalkoxysilane on efficiency and selectivity of the photocatalytic process. The photoactivity of $Na_4W_{10}O_{32}/SiO_2$ and $Na_4W_{10}O_{32}/SiO_2$/BTESE is also compared with that shown by $Na_4W_{10}O_{32}$ dissolved in water in

order to investigate the role of textural features and surface properties of the solid supports in tuning the photocatalytic activity of the decatungstate.

2. Experimental

2.1 Photocatalysts preparation and characterization

Reagents and solvents were purchased from Sigma in the highest purities available and used without further purification. Sodium decatungstate ($Na_4W_{10}O_{32}$) was synthesised as reported in the literature [33]. The heterogeneous photocatalyst ($Na_4W_{10}O_{32}/SiO_2$) was prepared by hydrolysis of tetraethyl orthosilicate (TEOS, 23 mmol, 4.8 g) in the presence of an acid aqueous solution of $Na_4W_{10}O_{32}$, following a procedure published in detail for the entrapment of $(nBu_4N)_4W_{10}O_{32}$ inside silica [27]. $Na_4W_{10}O_{32}/SiO_2$/BTESE has been obtained by the simultaneous hydrolysis of TEOS (23 mmol, 4.8 g) and BTESE (2.3 mmol, 0.8 g) . On the basis of the solid mass obtained at the end of the preparation and the initial amount of $Na_4W_{10}O_{32}$ employed (0.5 g), we could estimate that both the prepared materials contained 30% (w/w) of decatungstate. UV-vis spectra of washing water aliquots showed that $Na_4W_{10}O_{32}$ was not released into the solution. A sample not including the polyanion (SiO_2) was also prepared carrying out the hydrolysis in the absence of decatungstate.

Diffuse reflectance UV-vis spectra were recorded with a Jasco V-570 using an integrating sphere and $BaSO_4$ as reference. The plotted spectra were obtained by the Kubelka-Munk transformation ($F(R) = 1 - R^2/2R$) versus the wavelengths. FTIR spectra were obtained by means of Bruker IFS28, Globar source and cryodetector MCT with resolution 4 cm^{-1}. The spectra were obtained in home-made vacuum cell allowing the outgassing of the material (residual pressure of 10^{-4} mbar) and the simultaneous spectroscopic measurement. Materials were prepared in form of self-supporting pellets (~ 40 g/cm^2) and in form of thin layers (~ 10 g/cm^2) supported on silicon wafer.

N_2 adsorption-desorption experiments were carried out at 77 K by means of ASAP2020 instrument (Micromeritics). Before each measurement, samples were outgassed overnight at 150 °C with a rotative pump (residual pressure about 10^{-2} mbar).

Microgravimetric adsorption isotherms were obtained at 25°C with microbalance apparatus (IGA002 by Hiden), contacting the powders with water and toluene vapours. The temperature control was guaranteed by thermostatic bath. Adsorption tests of toluene in liquid phase were also carried out by putting 100 mg of $Na_4W_{10}O_{32}/SiO_2$/BTESE or $Na_4W_{10}O_{32}/SiO_2$ in 0,2 mL of a water solutions containing toluene. The mixtures were rapidly stirred at room temperature for 30 min. The powder dispersions were, then, centrifuged and the solution analyzed by GC. Adsorbed toluene was quantified by its decrease in the solution after the contact with the solid.

EPR spin trapping experiments were carried out with a Bruker ER 200 MRD spectrometer equipped with a TE 201 resonator, at a microwave frequency of 9.4 GHz. The samples were constituted by suspensions of one of the two photocatalysts (20 mg) in 1 mL of aqueous solutions of 5,5-dimethylpyrroline *N*-oxide (DMPO 4 x 10^{-2} M) as spin trap, in the presence of toluene (6 x 10^{-3} M) when requested. Samples were put into a flat quartz cell and directly irradiated (λ>290 nm) inside the EPR cavity with a Helios Q400 Italquartz medium-pressure Hg lamp. No signals were obtained in the dark and during irradiation of the solution in the absence of photocatalyst.

Photocatalytic experiments

The photocatalysts $Na_4W_{10}O_{32}/SiO_2$/BTESE or $Na_4W_{10}O_{32}/SiO_2$ (100 mg) were kept in contact with 0.2 mL of a saturated water solution of toluene (6 x 10^{-3} M). After 10 minutes of stirring the powder suspension was centrifuged. The liquid phase was analyzed by gas chromatographic technique in order to establish the amount of toluene still present in the water phase. Then, the material containing toluene (100 mg) was suspended in 0.5 mL of distilled water and irradiated for 30 minutes inside a 3 mL spectrophotometric cell, upon stirring. Photochemical excitation was performed with a medium-pressure Hg lamp (like that described above). A glass cut-off filter was used for selecting light of wavelengths higher than 290 nm. Measurements with an ultraviolet radiometer indicated that this amount of photocatalyst absorbs more than 90% of the impinging radiation. At the end of the photocatalytic experiment, the sample was centrifuged and the aqueous phase analyzed by GC. The irradiated powder was also suspended in aliquots (0.2 mL) of water, acetone, acetonitrile and dichloromethane in order to extract all the products eventually entrapped. Homogeneous photocatalytic experiments were carried out dissolving $Na_4W_{10}O_{32}$ in a saturated water solution of toluene (3 mL). The decatungstate concentration in this solution (2 x 10^{-4} M) warranted the complete absorption of the incident photons. After irradiation, the samples were analyzed as described above.

Product analyses were carried out with a gas chromatograph HP 6890 Series Instrument equipped with a flame ionization detector and a HP-WAX (cross linked polyethylene glycol, 30 m, 0.32 mm x 0.5 μm film thickness) capillary column. The quantitative analyses were carried out with calibration curves obtained with authentic samples.

In order to establish the amount of CO_2 eventually formed, samples containing $Na_4W_{10}O_{32}/SiO_2$/BTESE or $Na_4W_{10}O_{32}/SiO_2$ were irradiated maintaining the reactor firmly closed. At the end of irradiation 2.6 mL of a NaOH solution (0.1 M) were put inside the reactor with a syringe and mixed with the irradiated dispersion. Then, after centrifugation, 2.0 mL of the aqueous phase were taken and kept into a vial. After the addition of 1 mL of saturated citric acid solution, carbon dioxide released was measured by pH-meter BasiC 20 CRISON equipped with a gas sensing

probe (Crison 9666). Quantitative analysis was made through a calibration curve built from standard solutions of $NaHCO_3$ treated as described above. Results obtained after irradiation were compared with those coming from analogous samples kept in the dark for the same period. The yield of CO_2 was referred to the number of carbon atoms present in a toluene molecule.

No oxidation products were observed when blank experiments were run in the dark. Other control experiments indicated that irradiation of saturated water solution of toluene in the presence of SiO_2 without decatungstate did not yield appreciable amounts of oxidation products.

Some experiments were carried out in order to test the stability of $Na_4W_{10}O_{32}/SiO_2$/BTESE in repeated photocatalytic experiments: an aliquot of 100 mg of photocatalyst has been recycled in subsequent photocatalytic experiments after washing with aliquots of water, acetone, acetonitrile and dichloromethane and drying at 373 K for 60 minutes.

Results and Discussion

Synthesis and textural characterization

Entrapment of $Na_4W_{10}O_{32}$ in a silica matrix for obtaining $Na_4W_{10}O_{32}/SiO_2$ photocatalyst has been carried out following a sol-gel procedure previously published [13]. Preparation of the $Na_4W_{10}O_{32}/SiO_2$/BTESE material is based on the use of BTESE, which hydrolyzes together with TEOS [28, 30, 31]. The preparation of both $Na_4W_{10}O_{32}/SiO_2$/BTESE and $Na_4W_{10}O_{32}/SiO_2$ is carried out at pH 2. At this pH value, the silanol groups ≡Si-OH are protonated to form ≡Si-OH_2^+. These species can act, in turn, as counterions for $W_{10}O_{32}^{4-}$ groups yielding the couple (≡Si-OH_2^+)($Na_3W_{10}O_{32}^-$) by acid-base reaction. The interaction established is very strong and the decatungstate groups are no longer released when these materials are dispersed in aqueous medium.

Fig 1 shows the UV-vis spectra of $Na_4W_{10}O_{32}/SiO_2$/BTESE and $Na_4W_{10}O_{32}/SiO_2$ (curves A and B, respectively). Spectra of $Na_4W_{10}O_{32}$ (curve C) and of silica support (curve D) are also reported for a sake of comparison. Both $Na_4W_{10}O_{32}/SiO_2$/BTESE and $Na_4W_{10}O_{32}/SiO_2$ present an intense absorption at wavelengths lower than 400 nm, due to the presence of decatungstate.

Figure 1.

Gas-volumetric adsorption of N_2 at low temperature gives important information about the morphological features of $Na_4W_{10}O_{32}/SiO_2$/BTESE system. As far as the surface specific area is concerned, we characterized this material by means of the BET method [34]. In order to evaluate the porosity eventually close in size to the boundary between micro and mesoporosity regions, we employ here the same method already adopted for the investigation of $Na_4W_{10}O_{32}/SiO_2$, which

bases on Density Functional Theory (DFT) [27]. Specific surface area and pore volume data of $Na_4W_{10}O_{32}/SiO_2$/BTESE are summarized in Table 1, compared with the results previously published for $Na_4W_{10}O_{32}/SiO_2$ [13]. The porosity data, whose relative pore size distributions are shown in Figure 2, are reported splitted in two contributions, micropores below 10 Å and mesopores above 10 Å of width, on the basis of materials pore distribution.

Table 1 shows that the specific surface area of $Na_4W_{10}O_{32}/SiO_2$/BTESE is markedly higher than that of its parent material $Na_4W_{10}O_{32}/SiO_2$. It is also seen that the introduction of the organoalkoxysilane enhances of about 40% the total pore volume. More specifically, this increase is essentially due to an increase of mesoporosity: in fact, $Na_4W_{10}O_{32}/SiO_2$/BTESE presents a larger amount of pores with width of 13 and 28 Å. These results indicate that the incorporation of BTESE during the synthesis of the silica-based material induces important modification to the porous texture of this material, suggesting that the organoalkoxysilane can act as a templating agent.

Figure 2.

Surface effects.

Some experiments have been carried out in order to compare adsorption of water and toluene on $Na_4W_{10}O_{32}/SiO_2$/BTESE and $Na_4W_{10}O_{32}/SiO_2$. As shown in Figure 3, water vapour is better adsorbed on the surface of $Na_4W_{10}O_{32}/SiO_2$, whereas the adsorption observed on $Na_4W_{10}O_{32}/SiO_2$/BTESE is more limited. It suggests that the synthesis with BTESE makes the surface of silica more hydrophobic, as observed for other similar materials [29, 31]. This is confirmed by FTIR spectra (Figure 4), obtained on self-supporting pellets (to observe CH signals) and on thin layers (to observe OH signals), indicating the presence of hydrocarburic fragments still present after calcination treatment. Analogously, also OH groups are still visible in the spectra, and they could be responsible for the not negligible interaction observed with water molecules. Therefore, the calcination temperature was not high enough to induce the complete removal of BTESE precursor and the elimination of silanols with subsequent formation of siloxane groups (Si-O-Si) [35].

Figure 3.

Figure 4

Toluene adsorption data confirm the hydrophobic character of $Na_4W_{10}O_{32}/SiO_2$/BTESE surface compared to $Na_4W_{10}O_{32}/SiO_2$ one. Toluene adsorption isotherms were obtained via microgravimetric analysis using toluene in vapour phase as adsorptive (Figure 5) and via GC from toluene aqueous solution (Figure 6). Analogous trends were obtained, although the extent of adsorption is dramatically enhanced in the case of adsorption from vapour phase. A possible explanation of this phenomenon can be ascribed to the size of molecules in gas and liquid phase and to the consequent ability to penetrate in the void space (pores) of materials: in the gas phase, the naked molecules can interact more easily than in the corresponding solvated situation.

Figure 5.

Figure 6.

Hydroxyl radicals formation

EPR spin-trapping investigation is a powerful technique for detecting the formation of short-lived radicals and has been fruitfully employed in photochemical studies on polyoxometalates in order to better understand photochemical primary processes [13, 14, 36, 37]. The technique is based on the ability of some molecules, such as nitrones, to trap radicals to give nitroxides stable enough to be successfully detected and characterized. The nature of the trapped radical can be often identified by the parameters obtainable from the EPR spectrum.

Evidences of the formation of $OH^{\bullet}$ radicals as a consequence of photoexcitation of $Na_4W_{10}O_{32}/SiO_2$ in aqueous system were previously obtained using 5,5-dimethylpyrroline *N*-oxide (DMPO) as a spin trap [13, 14]. This species is able to react with $OH^{\bullet}$ radicals according to Eq. 2 to form the paramagnetic adduct $[DMPO\text{-}OH]^{\bullet}$, whose typical spectrum consists of a quartet 1:2:2:1 ($a_N = a_H = 14.5$ gauss) [38]. The formation of $OH^{\bullet}$ radicals in that photocatalytic system were ascribed to both the direct water oxidation (Eq. 1) and the reaction between the photogenerated $W_{10}O_{32}^{5-}$ and H_2O_2 (Eq. 3), which must be included among the products of the reoxidation process of $W_{10}O_{32}^{5-}$ by O_2 [14].

$$DMPO + OH^{\bullet} \longrightarrow [DMPO\text{-}OH]^{\bullet} \qquad (2)$$

$$H_2O_2 + W_{10}O_{32}^{5-} \longrightarrow W_{10}O_{32}^{4-} + OH^{\bullet} + OH^{-} \qquad (3)$$

The EPR spin-trapping investigation indicates that $OH^{\bullet}$ radicals are formed also as a consequence of photoexcitation of $Na_4W_{10}O_{32}/SiO_2/BTESE$. In fact, Fig. 7 shows that illumination ($\lambda > 290$ nm) of this material in aqueous suspensions containing DMPO (4×10^{-2} M) causes the prompt formation of a quartet whose signal pattern and coupling constant values are in agreement with the trapping of $OH^{\bullet}$ radicals by DMPO, according to Eq. 2 [38]. Control experiments show that no signal is observed neither in the dark nor during irradiation in the absence of photocatalyst.

Figure 7.

Figure 8a compares the intensity of the $[DMPO\text{-}OH]^{\bullet}$ adduct in time upon irradiation of $Na_4W_{10}O_{32}/SiO_2/BTESE$ in the absence and in the presence of toluene. The addition of toluene causes a strong decrease of the intensity of the EPR signal, indicating that this molecule is a very good competitor for the reaction with $OH^{\bullet}$ radicals in respect to the spin trap species. This is not surprising considering that adsorption phenomena on the hydrophobic surface of $Na_4W_{10}O_{32}/SiO_2/BTESE$ favour the access of toluene into the silica framework in proximity of the photoactive decatungstate. Accordingly, the presence of toluene does not cause appreciable changes in the $[DMPO\text{-}OH]^{\bullet}$ signal intensity during irradiation of the more hydrophilic $Na_4W_{10}O_{32}/SiO_2$ photocatalyst, as indicated by the curves reported in Figure 8b.

Figure 8.

Toluene entrapment and photodegradation

Continuous irradiations of $Na_4W_{10}O_{32}/SiO_2$ and $Na_4W_{10}O_{32}/SiO_2/BTESE$ systems in toluene saturated water solutions have been carried out in order to investigate the reactivity of the photogenerated $OH^{\bullet}$ radicals. Likely, these oxidizing species can be able to initiate toluene oxidation that, upon aerobic conditions, leads to the formation of oxygenated products and, finally, to the complete mineralization to carbon dioxide and water.

Before photochemical excitation, $Na_4W_{10}O_{32}/SiO_2/BTESE$ or $Na_4W_{10}O_{32}/SiO_2$ (100 mg) were contacted with 0.2 mL of toluene saturated water solution (6×10^{-3} M, see experimental part). Table 2 shows that, after 10 minutes, about all the toluene present in solution was entrapped by $Na_4W_{10}O_{32}/SiO_2/BTESE$, whereas, in line with the adsorption measurements reported in Figures 5 and 6, $Na_4W_{10}O_{32}/SiO_2$ entrapped toluene in a significantly lower degree (about 54%). Each

photocatalytic material containing toluene was then suspended in distilled water (0.5 mL) and irradiated ($\lambda > 290$ nm) for 30 minutes. Measurements with an ultraviolet radiometer indicated that the employed amount of photocatalyst absorbs more than 90% of the impinging radiation. Table 2 reports nature and yields of the detected products.

Table 2.

$Na_4W_{10}O_{32}/SiO_2$/BTESE shows high efficiency and a very strong oxidizing ability. In fact, only 5.8% of the adsorbed toluene remained after irradiation and 91.8% of the disappeared toluene was converted to CO_2. $Na_4W_{10}O_{32}/SiO_2$ shows a minor efficiency: in fact, 18.3 % of the adsorbed toluene is recovered after irradiation. Besides CO_2, minor amounts of benzyl alcohol and benzaldehyde are also formed. Control experiments indicate that no oxidation product was formed in detectable amount in the absence of light or irradiating the raw silica materials without decatungstate. Moreover, no CO_2 was formed irradiating $Na_4W_{10}O_{32}/SiO_2$/BTESE in the absence of toluene, indicating that the organic part of BTESE does not undergo degradation during the photocatalytc experiment.

The strong mineralizing ability of the photocatalytic materials is in line with EPR spin-trapping findings, that evidence the formation of $OH^{\bullet}$ radicals. These powerful and unselective oxidants are formed in the constrained environment of the photocatalysts pores, where restrictions of molecular motion may favor over-oxidation of the primary photoproducts (benzyl alcohol and benzaldehyde) to CO_2. This explanation is further supported by the findings obtained irradiating $Na_4W_{10}O_{32}$ (2×10^{-4} M, 30 min, $\lambda > 290$ nm) dissolved in toluene saturated water solutions. In this case, only 8% of initial toluene is converted to CO_2 indicating that in these conditions primary oxidation products are free to diffuse going away the photoactive decatungstate so preventing their subsequent oxidation.

The data of Table 2 show that the amount of benzyl alcohol entrapped within the two photocatalysts is different: as expected on the basis of hydrophobicity characteristics of the two photocatalysts, only 34% of formed alcohol is adsorbed by $Na_4W_{10}O_{32}/SiO_2$/BTESE while 63% of benzyl alcohol remained in the hydrophilic $Na_4W_{10}O_{32}/SiO_2$. Therefore, the adsorbed alcohol can easily react with the photoexcited decatungstate and converted to benzaldehyde. This is confirmed considering the ratios between μmoles of benzaldehyde and benzyl alcohol with the two photocatalysts. It is seen that the ratio is 3.2 for $Na_4W_{10}O_{32}/SiO_2$/BTESE and increases up 8.7 for $Na_4W_{10}O_{32}/SiO_2$.

Efficiency of a photocatalyst is usually evaluated also in terms of its stability. $Na_4W_{10}O_{32}/SiO_2/BTESE$ can be reused for further reaction. In fact, after the first photocatalytic experiment, it was recovered, washed with water, acetone, acetonitrile and dichloromethane sequentially, and used again in a second experiment without any loss of activity.

Conclusions

A new photocatalytic material has been prepared by entrapment of $Na_4W_{10}O_{32}$ inside porous organosilica. This material is able to scavenge and to accumulate significant amounts of toluene from toluene saturated water solutions. This is due to the large surface area of $Na_4W_{10}O_{32}/SiO_2/BTESE$, presence of micro and mesopores and, especially, to the hydrophobicity of its surface. Photoexcited $Na_4W_{10}O_{32}/SiO_2/BTESE$ shows a very high efficiency since it adsorbs all the toluene present in solution and converts more than 90% of the adsorbed hydrocarbon to CO_2. Likely, micro and mesopores cooperate to the photodegradation, since they can act as small microreactors, where both restriction of molecular motions and high hydrophobicity increase the contact between toluene (and its oxidized intermediates) and photoactive decatungstate groups. The close interaction favors the reaction of substrate with the photogenerated $OH^{\bullet}$ radicals to yield CO_2 as final main degradation product. A comparison with the photocatalytic activity of $Na_4W_{10}O_{32}$ dissolved in homogeneous solution confirms that textural effects can critically affect the oxidation properties of the decatungstate. Finally, the photocatalyst $Na_4W_{10}O_{32}/SiO_2/BTESE$ is robust and reusable without loss of activity. The above conclusions may open new perspectives for developing new efficient and stable photocatalytic systems addressed to clean wastewater containing aromatic hydrocarbons.

References

1) A. Hiskia, A. Mylonas, E. Papaconstantinou, Chem. Soc. Rev., 30 (2001) 62-69.
2) A special issue of Chemical Reviews is devoted to polyoxometalates: C. L. Hill Ed., Chem. Rev., 98 (1998).
3) A. Maldotti, A. Molinari, R. Amadelli, Chem. Rev., 102 (2002) 3811-3836.
4) A. Maldotti, A. Molinari, Top. Curr. Chem, 303 (2011) 185-216.
5) A. M. D. Tzirakis, I. N. Lykakis, M. Orfanopoulos, Chem. Soc Rev., 38 (2009) 2609-2621.
6) C. Tanielian, Coord. Chem. Rev., 178-180 (1998) 1165-1181.
7) C. Tanielian, I. N. Lykakis, R. Seghrouchni, F. Cougnon, M. Orfanopoulos, J. Mol. Catal. A: Chem., 262 (2007) 170-175.
8) I. N. Lykakis, M. Orfanopoulos, Tetrahedron Lett., 46 (2005) 7835-7839.
9) P. Kormali, A. Troupis, T. Triantis, A. Hiskia, E. Papaconstantinou, Catal. Today, 124 (2007) 149-155.
10) D.C. Duncan, M.A. Fox, J. Phys. Chem. A, 102 (1998) 4559-4567.
11) Y. Yamase, Inorg. Chim. Acta, 76 (1983) L25-L26.
12) A. Mylonas, A. Hiskia, E. Androulaki, D. Dimotikali, E. Papaconstantinou, Phys. Chem. Chem. Phys, 1 (1999) 437-440.
13) A. Molinari, A. Maldotti, A. Bratovcic, G. Magnacca, Catal. Today, doi:10.1016/j.cattod.2011.11.033
14) A. Molinari, R. Argazzi, A. Maldotti, J. Mol. Catal. A: Chem., submitted.
15) A. Maldotti, A. Molinari, G. Varani, M. Lenarda, L. Storaro, F. Bigi, R. Maggi, A. Mazzacani, G. Sartori, J. Catal., 209 (2002) 210-216.
16) A. Molinari, G. Varani, E. Polo, S. Vaccari, A. Maldotti, J. Mol. Catal. A: Chem., 262 (2007) 156-163.
17) A. Maldotti, A. Molinari, F. Bigi, J. Catal., 253 (2008) 312-317.
18) M. Bonchio, M. Carraro, G. Scorrano, A. Bagno, Adv. Synth. Catal., 345 (2003) 1119-1126.
19) M. Carraro, M. Gardan, G. Scorrano, E. Drioli, E. Fontananova, M. Bonchio, Chem. Commun., (2006) 4533-4535.
20) Y. Guo, C. Hu, J. Mol. Catal. A: Chem., 262 (2007) 136-148.
21) Y. Guo, D. Li, C. Hu, E. Wang, Y. Wang, Y. Zhou, S. Feng, Appl. Catal. B: Environ, 30 (2001) 337-349.
22) H. Y. Shen, H. L. Mao, L. Y. Ying, Q. H. Xia, J. Mol. Catal. A:Chem., 276 (2007) 73-79.
23) S. Anadan, S. Y. Ryu, W. Cho, M. Yoon, J. Mol. Catal. A: Chem., 195 (2003) 201-208.
24) R. R. Ozer, J. L. Ferry, J. Phys. Chem. B, 106 (2002) 4336-4342.
25) L. Ni, J. Ni. Y. Lv, P. Yang, Y. Cao, Chem. Commun., (2009) 2171-2173.
26) S. Farhadi, M. Zaidi, Appl. Catal., A: Gen., 354 (2009) 119-126.
27) A. Molinari, A. Bratovcic, G. Magnacca, A. Maldotti, Dalton Trans., 39 (2010) 7826-7833.
28) M. Kapoor, A. Bhaumik, S. Inagaki, K. Kuraoka, T. Yazawa, J. Mater. Chem. 12 (2002) 3078-3083.
29) A. Bhaumik, M. P. Kapoor, S. Inagaki, Chem. Commun., (2003) 470-471.
30) Y. Shiraishi, H. Ohara, T. Hirai, J. Catal. 254 (2008) 365-373.
31) Y. Shiraishi, H. Ohara, T. Hirai, New J. Chem., 34 (2010) 2841-2846.
32) G. Marci, M. Addamo, V. Augugliaro, S. Coluccia, E. Garcia-Lopez, V. Loddo, G. Martra, L. Palmisano, M. Schiavello, J. Photochem. Photobiol. A: Chem, 160 (2003) 105-114.
33) F. Bigi, A. Corradini, C. Quarantelli, G. Sartori, J. Catal., 250 (2007) 222-230.
34) S. Brunauer, P.H. Emmet, E. Teller, J. Am. Chem. Soc, 60 (1938) 309-319.
35) M. Morishita, Y. Shiraishi, T. Hirai, J. Phys. Chem. B, 110 (2006) 17898-17905.
36) A. Molinari, M. Montoncello, H. Rezala, A. Maldotti, Photochem. Photobiol. Sci., 8 (2009) 613-619.
37) D. Dondi, D. Ravelli, M. Fagnoni, M. Mella, A. Molinari, A. Maldotti, A. Albini, Chem. Eur. J. 15 (2009) 7949-7957.

38) E.G. Janzen, Acc. Chem. Res. 4 (1971) 31-40.

Captions

Figure 1. DR-UV-vis spectra of $Na_4W_{10}O_{32}/SiO_2$/BTESE (curve A), $Na_4W_{10}O_{32}/SiO_2$ (curve B), $Na_4W_{10}O_{32}$ (curve C) and SiO_2 (curve D).

Figure 2. DFT pore analysis for $Na_4W_{10}O_{32}/SiO_2$/BTESE (solid line) and $Na_4W_{10}O_{32}/SiO_2$ (broken-line).

Figure 3. Microgravimetric adsorption isotherms of water vapour on $Na_4W_{10}O_{32}/SiO_2$ (●) and $Na_4W_{10}O_{32}/SiO_2$/BTESE (■) activated at 25°C. The adsorption experiments were carried out at 25°C.

Figure 4. FTIR spectra relative to $Na_4W_{10}O_{32}/SiO_2$ (curve a) and $Na_4W_{10}O_{32}/SiO_2$/BTESE (curve b). Curves a' and b' refer to the same samples in form of thin layers (deposition on Si wafer). The arrows in the figure indicate the main signals due to the modifier (ν_{CH} at 2900 and δ_{CH} at 1412 cm^{-1}) and to silica hydroxyls (ν_{OH} at 3730 cm^{-1}).

Figure 5. Microgravimetric adsorption isotherms of toluene vapour on $Na_4W_{10}O_{32}/SiO_2$ (●) and $Na_4W_{10}O_{32}/SiO_2$/BTESE (■) activated at 25°C. The adsorption experiments were carried out at 25°C.

Figure 6. Toluene adsorption isotherms from liquid phase on $Na_4W_{10}O_{32}/SiO_2$/BTESE (■) and $Na_4W_{10}O_{32}/SiO_2$ (●).

Figure 7. EPR spectrum of $[DMPO\text{-}OH]^{\bullet}$ obtained upon irradiation (λ>290 nm) of $Na_4W_{10}O_{32}/SiO_2$/BTESE dispersed in water containing DMPO (4×10^{-2} M).

Figure 8. Fixed-field signal intensity of the $[DMPO\text{-}OH]^{\bullet}$ adduct in time upon irradiation (λ>290 nm) of: (a) $Na_4W_{10}O_{32}/SiO_2$/BTESE dispersed in water containing DMPO (4×10^{-2} M, full squares) and in an analogous solution containing also toluene (6×10^{-3} M, empty squares), (b) $Na_4W_{10}O_{32}/SiO_2$ dispersed in water containing DMPO (4×10^{-2}M, full circles) and in an analogous solution containing also toluene (6×10^{-3} M, empty circles).

Table(s)

Table 1. Morphological features of $Na_4W_{10}O_{32}/SiO_2$ and of $Na_4W_{10}O_{32}/SiO_2$/BTESE.

Sample	SSA (m^2g^{-1})	V_{tot} (cm^3g^{-1})	V_{micro} (< 10 Å width, cm^3g^{-1})	V_{meso} (> 10 Å width, cm^3g^{-1})
$Na_4W_{10}O_{32}/SiO_2$	521	0.25	0.08	0.17
$Na_4W_{10}O_{32}/SiO_2$/BTESE	725	0.35	0.06	0.29

Table(s)

Table 2. Photocatalytic oxidation of toluene by $Na_4W_{10}O_{32}/SiO_2$/BTESE and $Na_4W_{10}O_{32}/SiO_2$[a]

Total μmoles of reagents and products *(μmoles of reagents and products entrapped within the photocatalyst)* [% with respect to adsorbed toluene μmoles]		
Reagents and products	$Na_4W_{10}O_{32}/SiO_2$/BTESE	$Na_4W_{10}O_{32}/SiO_2$
Toluene before irradiation	1.20 *(1.20)*	1.20 *(0.65)*
Toluene after irradiation	4.8×10^{-2} *(2×10^{-2})* [5.8 %]	7.6×10^{-2} *(4.3×10^{-2})* [18.3 %]
CO_2 [b]	1.1 [91.8 %]	0.5 [77 %]
Benzyl alcohol	4.7×10^{-3} *(1.6×10^{-3})* [0.6 %]	1.9×10^{-3} *(1.2×10^{-3})* [0.5 %]
Benzaldehyde	1.1×10^{-2} *(0.9×10^{-2})* [1.8 %]	1.6×10^{-2} *(1.1×10^{-2})* [4.2 %]

[a] In a typical experiment, $Na_4W_{10}O_{32}/SiO_2$/BTESE or $Na_4W_{10}O_{32}/SiO_2$ (200 g/L) were contacted with toluene saturated water solution,,then irradiated in distilled water ($\lambda > 290$ nm) for 30 min at 25 $\pm$ 1°C and 1 atm of O_2. Reported values are the mean of three repeated experiments (percentual error is $\pm$5%).

[b] The yield of CO_2 was referred to the number of carbon atoms present in a toluene molecule.

Figure(s)

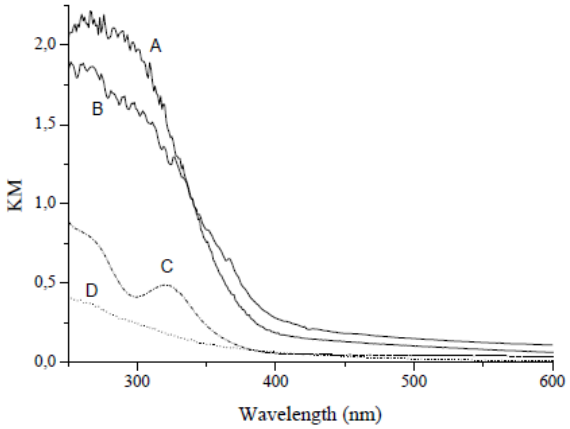

Figure 1.

Figure(s)

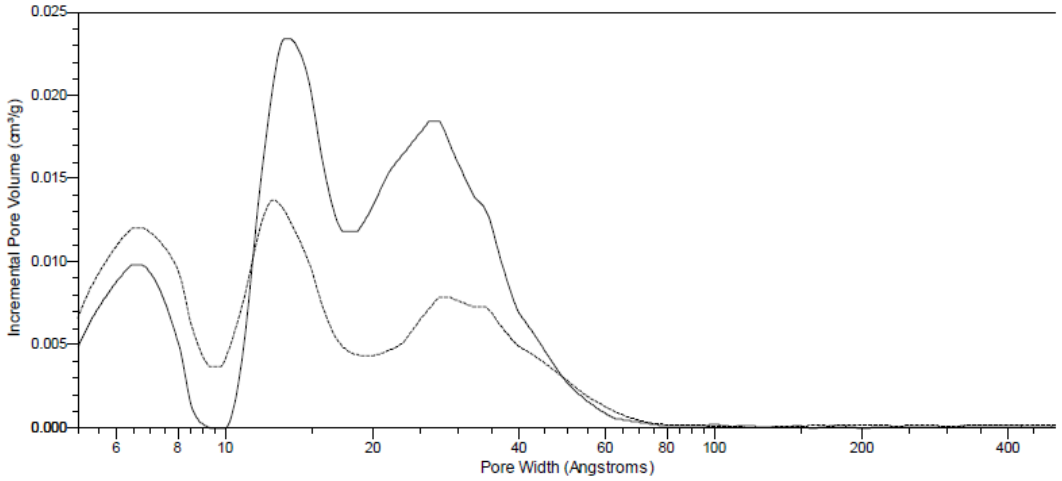

Figure 2

Figure(s)

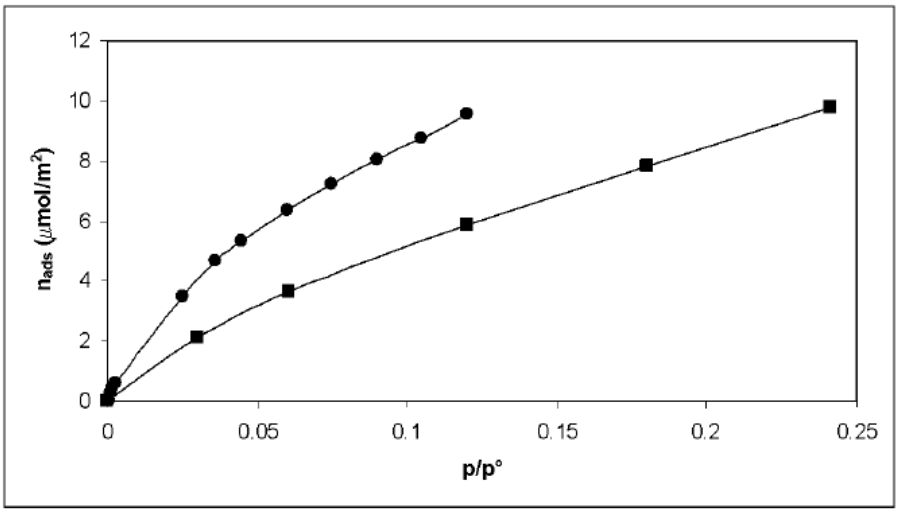

Figure 3.

Figure(s)

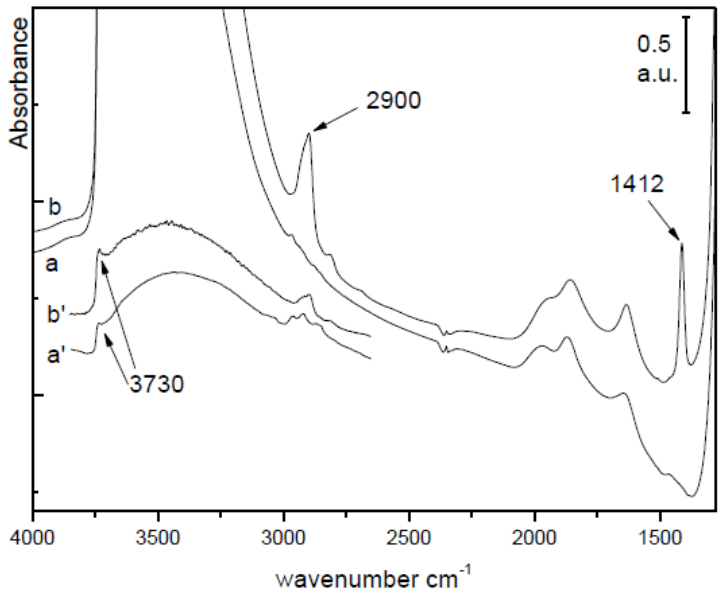

Figure 4.

Figure(s)

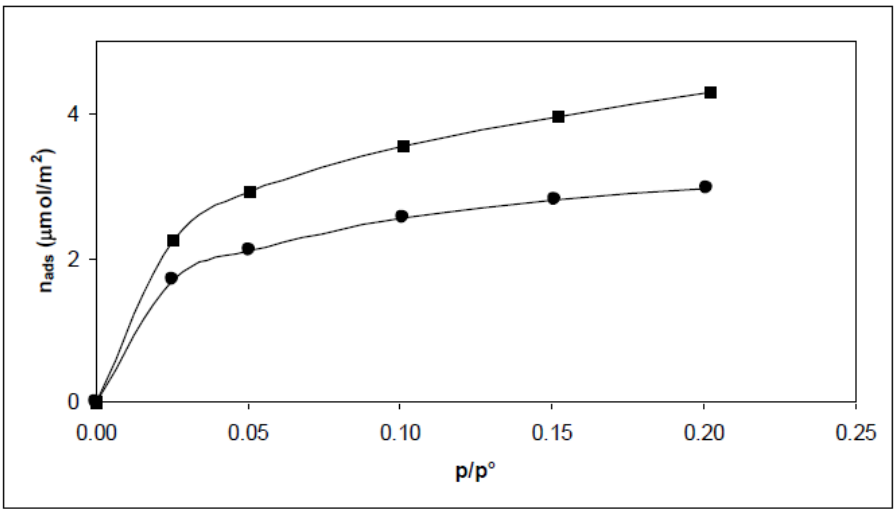

Figure 5

Figure(s)

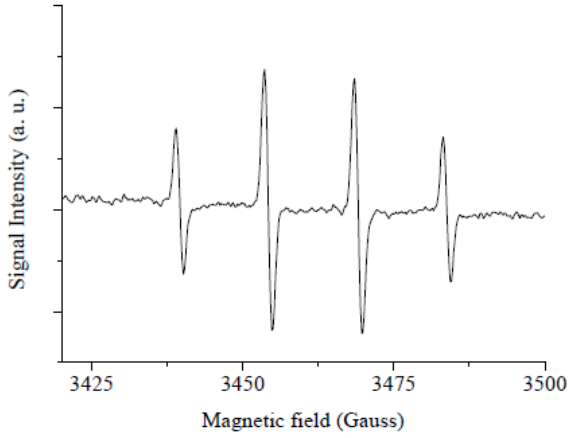

Figure 7